JOURNAL OF MATERIALS SCIENCE 19 (1984) 457–466

High temperature fracture of boron carbide: experiments and simple theoretical models

G. DE WITH
Philips Research Laboratories, POB 80000, 5600 JA, Eindhoven, The Netherlands

The mechanical properties of theoretically dense boron carbide with a grain size of about 10 μm have been investigated as a function of temperature. It was found that the fracture toughness remained constant at ~ 3.7 MPa $m^{1/2}$ up to 1500 K and there was little or no decrease in strength from its room temperature value of ~ 350 MPa. Both the order of magnitude and the temperature dependence of the fracture energy, calculated from the fracture toughness and elastic data, can be explained in terms of simple theoretical models.

1. Introduction

Boron carbide (B_4C) is an important ceramic material which is used in lightweight armour for the armed forces, as a neutron absorber in nuclear reactors and as an abrasive material for grinding and/or polishing operations. In view of its refractory nature, high temperature applications are also within reach. In the latter case the material usually has to endure (thermo-)mechanical loads as well. Furthermore, since bonding in B_4C is covalent and the material is available in a dense and rather pure form, it seems to be a proper material for analysis of its fracture behaviour. As little has been hitherto reported about the fracture behaviour of B_4C at elevated temperatures, an investigation into this behaviour was conducted. A useful general review on B_4C dealing with structure, properties and some applications is given in [1].

2. Experimental details

The B_4C ceramic used is a commercially available hot-pressed material* with a purity of at least 99%. Major impurities are given by the supplier to be iron (0.1 wt%) and silicon (0.1 wt%). The density of the material, ρ, was determined using Prokic's method [2]. The material was polished using 2–4 μm diamond powder and then etched electrolytically (3 A cm^{-2} in 1% KOH/H_2O for 3 sec) to reveal the microstructure. The grain size d was measured using Mendelson's method [3] counting about 200 grains. Strength, σ_f and fracture toughness, K_{1c}, specimens (1 mm x 3 mm x 15 mm) were machined from the available material by spark erosion. This small type of specimen makes efficient use of the material available, while retaining reliability [4]. The machining manner was such that the fracture plane of each specimen was parallel to the direction of hot pressing. In the specimens used for the K_{1c} measurements a notch with a width of $\sim 60\,\mu$m and a relative depth of ~ 0.15 was machined. Each specimen was precracked using a Knoop hardness indentation (2 N load) on both sides of the specimen at the notch root. Strength and fracture toughness measurements were carried out up to 1500 K in a dry, N_2 gas atmosphere (flow rate $\sim 10\,\ell\,mm^{-1}$, humidity ~ 200 ppmV H_2O) using a all-ceramic three-point bending rig (span 12 mm) in a Pt-resistance furnace. Each specimen was held at the testing temperature for about 15 min before fracturing. The crosshead speed of the testing machine† was 0.1 mm min^{-1} throughout. This corresponded to a strain rate of about 2×10^{-4} sec^{-1} [5]. In the calculated K_{1c} value the compliance factor as given by Brown and Srawley [6] was used. The strength was calculated using the "mechanics of materials" formula [7]. Five

*Tetrabor, Electroschmelzwerk Kempten G.m.b.H.
†Overload Dynamics S200.

0022–2461/84 $03.00 + .12

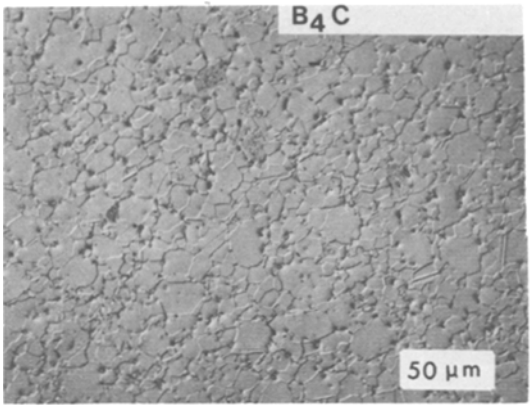

Figure 1 Micrograph of the B_4C using optical microscopy with interference contrast.

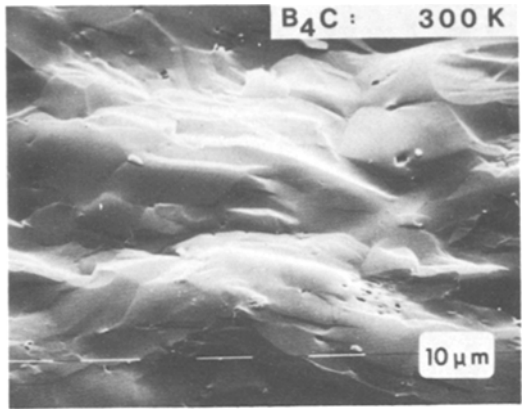

Figure 2 Fractograph of the B_4C using scanning electron microscopy. The fracture mode is entirely transgranular (also at higher temperatures) while the residual pores are generally found in clusters.

specimens were used in the K_{1c} determinations at each test temperature; likewise for the σ_f determinations, except at room temperature where nineteen specimens were used. Analysis of the strength data involved a least squares fit of the linearized Weibull equation, assuming zero threshold stress and using mean rank fracture probabilities [7, 8].

Specimens were etched in fuming $K_2S_2O_7$ (1000 K), initially resulting in an etching rate of about $3\,\mu m\,min^{-1}$ and in a somewhat smaller rate at longer etching times. Etching depths up to about $120\,\mu m$ were used. On average eight specimens were used for the strength measurement of the etched material.

The longitudinal wave velocity, v_l, and the shear wave velocity, v_s, were measured at 10 and 20 MHz, respectively, using the pulse-echo method* [9]. Young's modulus, E, and Poisson's ratio, ν, were calculated from v_l, v_s and ρ according to the usual formulae for isotropic materils [9]. No correction was made for attenuation.

Scanning electron microscope (SEM) photographs were taken of the fracture surface and a machined surface of a specimen fractured at each temperature and an etched surface at each etching depth. The roughness of the fracture surface was determined using a Tencor alpha step profiler (stylus tip radius $2\,\mu m$, magnification 2500×, scanned length $4800\,\mu m$). The compositions of the machined surfaces of the specimens fractured at 300 and 1500 K were determined by X-ray photo electron spectroscopy† (XPS); (Al$K\alpha$ radiation, overall spectra 500 to 1500 eV, pressure 10^{-6} Pa).

3. Results and discussion

In this section the material characteristics, fracture toughness, strength, and surface morphology are discussed and compared with other available data.

3.1. Material characteristics

The density of the material used was $2.51 \times 10^3\,kg\,m^{-3}$. The theoretical density of B_4C is $2.52 \times 10^3\,kg\,m^{-3}$ [14, 16], hence the material used has a relative density of 99.6%. A grain size of $10\,\mu m$ with a fairly regular distribution was observed. A micrograph is shown in Fig. 1. The remaining pores are generally found in clusters. This can clearly be seen in both the micrograph (Fig. 1) and the fractograph (Fig. 2). Further, a number of twinned grains was observed. These two characteristics have been dealt with in earlier literature [10, 11].

The values of the longitudinal wave velocity as measured parallel and perpendicular to the hot-pressing axis were the same within experimental error (~ 0.2%). Hence very little or no crystallographic texture was present.

The value of Young's modulus was 461 GPa, while Poisson's ratio equalled 0.178. A comparison with previous determinations of the E and ν of dense B_4C is given in Table I. A fairly good agreement amongst the different values of E is observed,

*Panametrics 5223.
†Leybold Heraeus LHS10.

TABLE I Elastic properties of B_4C at room temperature

ρ (g cm^{-3})	p*	d(μm)†	E(GPa)	ν	Remarks	References
–	0.004	2–7	453‡	0.14 (ass.)	resonance	12
–	0.004	–	444§	–	–	13
2.52 (ass.)	0.004	7.4	461¶	0.143	resonance	14
–	–	20	450	–	–	15
2.50	–	–	434	0.188	–	16
2.51	–	10	458 (static)	0.17	–	17
2.51	–	10	446 (dynamic)	0.17	–	17
2.46	0.016	0.1–1.0	383	–	3-point bend	18
2.51	0.005	5	441	0.17	resonance	19
2.4	–	1–3	480	–	resonance	20
2.51	0.004	10	461	0.178	pulse echo	this work

*p = porosity.
†d = grain size.
‡Calculated from $E = 460\ [(1-p)/(1+2.99p)]$ GPa.
§Calculated from $E = (450 - 7.24 \times 10^{-3} \times T - 3.88 \times 10^{-6} \times T^2)\ [(1-p)/(1+2.13p)]$ (T = temperature in ° C).
¶Calculated from $E = 470\ (1-4.58\ p)$ GPa.

except for the value determined with a bending test. The values of ν split into two groups: one centred around $\nu \approx 0.14$ and one about $\nu \approx 0.18$. Our measurement falls within the latter group.

3.2. Fracture toughness

The values of K_{1c} at the various testing temperatures are presented in Fig. 3. K_{1c} is roughly constant up to 1500 K at a value of 3.7 MPa m$^{1/2}$. The fracture mode was entirely transgranular at all testing temperatures (Fig. 2). A comparison with other relevant experimental values at room temperature is given in Table II.

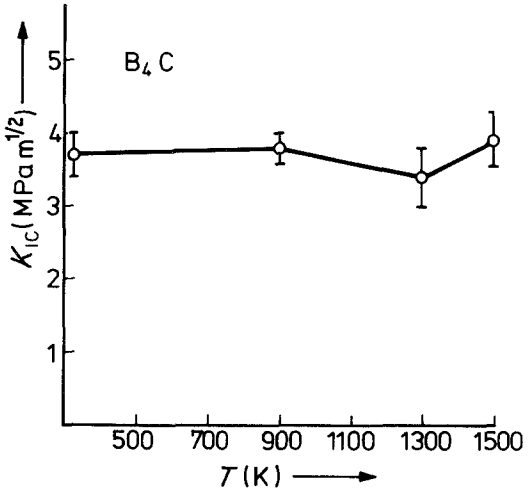

Figure 3 Fracture toughness of the B_4C as a function of temperature. Bars at the data points indicate the sample standard deviation.

Three other experimental values for the fracture toughness are found in the literature. A value of 1.9 MPa m$^{1/2}$ was determined by Hollenberg‡ [13] using the double torsion technique. Mecholsky *et al.* [15] determined a value of about 3.7 MPa m$^{1/2}$ using the double cantilever beam technique and Schwetz *et al.* [19] recently reported a value of 3.6 MPa m$^{1/2}$ using the single edge notched beam test. Our value (3.67 MPa m$^{1/2}$) compares favourably with the two latter values.

Calculation of the fracture energy, γ, [7] according to $\gamma = K_{1c}^2(1-\nu^2)/2E$ and K_{1c} values from the data groups $K_{1c} = 1.9$ MPa m$^{1/2}$ and $K_{1c} = 3.7$, 3.6 and 3.67 MPa m$^{1/2}$ results in $\gamma \sim 4$ J m^{-2} and $\gamma \sim 14$ J m^{-2}, respectively, for the two groups of data. An estimate of γ using a bond energy model usually yields a good order of magnitude for covalently bonded materials. In this case it yields $\gamma = 11.8$ J m^{-2} (see Appendix I). Since this calculation assumes a flat macroscopic fracture surface an additional macroscopic roughness factor has to be taken into account. The profilometer measurements resulted in $l/l_p = 1.013 \pm 0.004$. Here l and l_p represent the "true" and "projected" length of a fracture line, respectively. From l/l_p the fraction "flat" fracture area F [24] is calculated according to $F = (\pi(l/l_p) - 4)/(\pi - 4) = 0.95$. The ratio " true" area/"projected" area A/A_p is given by $A/A_p = 2 - F = 1.05$. Hence the calculated fracture energy should be multiplied by this small correction factor. The resulting value for γ is 12.4 J m^{-2}. Comparing this with the exper-

‡Hollenberg presents γ values calculated from E and K_{1c}, but neglects the thickness effect in the calculation of the K_{1c} from the double torsion formula. The inclusion of this correction yields the K_{1c} value quoted above.

TABLE II Fracture properties of B_4C at room temperature

ρ(g cm^{-3})	p*	d(μm)†	σ_f(MPa)	Remarks	K_{1c}(MPa m$^{1/2}$)	Remarks	References
–	0	2–7	–	–	1.77‡	DT,//	12
–	0.01	–	345	MOR	–	–	13
"theoretically dense"	0	2	510	4 pb	–	–	21
"theoretically dense"	0	16	430	4 pb	–	–	21
–	–	20	–	–	3.7	DCB (calculated from γ and E)	15
–	–	4.5	500	–	–	–	22
–	–	45	230	3 pb	–	–	22
2.51	–	10	330	4 pb	–	–	17
2.46	0.016	0.1–1.0	506	4 pb,//	–	–	18
–	0.02–0.03	8	320	ring test	–	–	23
2.51	0.005	5	480	4 pb	3.7	4 pb	19
2.51	0.004	10	382	3 pb, N_2	3.67	3 pb,//	this work

Abbreviations: DT = Double torsion, 3 pb = three-point bend, 4 pb = four-point bend, MOR = Modulus of Rupture, DCB = Double cantilever beam, // = fracture plane parallel to hot-pressing direction.
*p = porosity.
†d = grain size.
‡The results given in [2] should be corrected for specimen thickness. The corrected value would be 1.93 MPa m$^{1/2}$.

imental value of $\gamma \sim 14\,J\,m^{-2}$ good agreement is thus observed. On the other hand, the value of $\gamma \sim 4\,J\,m^{-2}$ as determined by Hollenberg and Walther [12] seems rather low.

The temperature dependence of γ can be calculated by differentiating $\gamma = K_{1c}^2(1-\nu^2)/2E$ while neglecting the temperature dependence of ν. This results in

$$\frac{1}{\gamma}\left(\frac{d\gamma}{dT}\right) = \frac{2}{K_{1c}}\left(\frac{dK_{1c}}{dT}\right) + \frac{1}{E}\left(\frac{dE}{dT}\right).$$

For the material used in this investigation K_{1c} was independent of temperature within experimental error. The temperature dependence of E for B_4C is known [13], which enabled us to calculate

$$\frac{1}{E(300\,K)}\left(\frac{dE}{dT}\right) = -2.6 \times 10^{-5}\,K^{-1}$$

and hence

$$\frac{1}{\gamma(300\,K)}\left(\frac{d\gamma}{dT}\right) = -2.6 \times 10^{-5}\,K^{-1}$$

Only one other determination of the temperature dependence of γ for B_4C has been found in the literature [12]. The material used in that investigation had a relative density of 92% and a grain size of 2–7 μm. An approximately linear decrease up to 1500 K was observed, with a relative decrease of

$$\frac{1}{\gamma(300\,K)}\left(\frac{d\gamma}{dT}\right) = -3.8 \times 10^{-4}\,K^{-1}.$$

Bearing in mind the similarity of the materials characteristics of these two materials, the results for $1/\gamma(d\gamma/dT)$ are in sharp contrast.

Aside from theoretical models dealing explicitly with surfaces, at least two semi-empirical models using bulk data are capable of estimating the value of $1/\gamma(d\gamma/dT)$. First, there is the "thermal" model (see Appendix II) which yields $1/\gamma(300\,K)\ (d\gamma/dT) = -2.6 \times 10^{-5}\,K^{-1}$, and secondly the "elastic" model (see Appendix III) yielding $1/\gamma(300\,K)\ (d\gamma/dT) = -1.8 \times 10^{-5}\,K^{-1}$. Both these theoretical values are in good agreement with each other and with the present experimental value and differ by one order of magnitude from the value deduced from the data of Hollenberg and Walther [12]. Note that both these models can be used without further corrections as the fracture mode is entirely transgranular.

3.3. Strength

The values of σ_f at the various testing temperatures are presented in Fig. 4. The strength σ_f decreases slightly from about 380 MPa at 300 K to about 340 MPa at 1500 K. Just as for the toughness measurements, the fracture mode was fully transgranular at all testing temperatures. A comparison with other experimental values at room temperature is again presented in Table II.

Values between ~300 and ~500 MPa are observed for the strength with the lower strength values corresponding to the larger grain sizes. The value of 382 MPa, as observed for B_4C at room

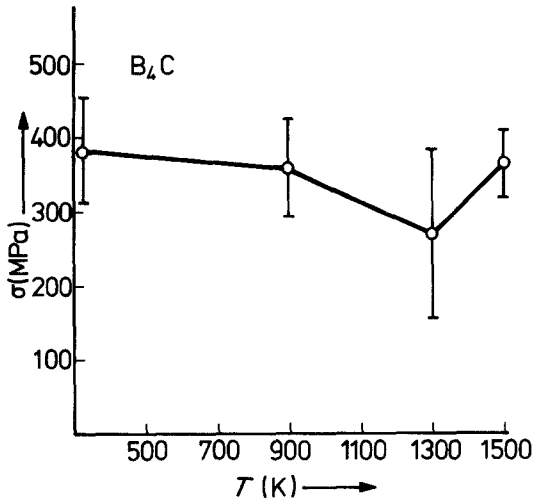

Figure 4 Strength of the B_4C as a function of temperature. Bars at the data points indicate the sample standard deviation.

temperature in this work, agrees favourably with the literature data.

The strength was observed to be highly variable as has been previously been reported [13]. The Weibull modulus m as calculated from the five specimens at each testing temperature was constant at a value of about 5. In order to establish the possible presence of a bi-modal flaw size distribution a Weibull analysis was made for the strength data measured at room temperature. Although the average strength calculated from the nineteen specimens ($\sigma_f = 354$ MPa) was somewhat smaller than that calculated from the original five specimens ($\sigma_f = 382$ MPa), the resulting Weibull modulus was again 5. Moreover, no indication of a bi-modal flaw size distribution was present in the Weibull plot. No characteristic differences could be found on the fracture surfaces either. Hence this wide flaw size distribution is probably inherent to the material.

Only one other determination of σ_f of B_4C at elevated temperatures has been found in the literature [13]. A decrease from about 345 MPa at 300 K to about 310 MPa at 1200 K is reported. The small decrease as observed in this work agrees nicely with these data.

A closer look at the temperature dependence of the mechanical properties reveals an increase in strength (Fig. 4) and to a much lesser extent also an increase in toughness (Fig. 3). This could be interpreted as due to plastic deformation since a testing temperature of 1500 K corresponds to about $0.55\,T_m$ (T_m = melting temperature ~ 2750 K [1]). At this magnitude of relative temperature plastic deformation generally commences. On the other hand the stress–strain curves were entirely linear up to 1500 K and no differences in fracture surfaces could be detected. Further it is known that the hardness of B_4C is still rather high (~ 20 GPa [25]) at 1500 K. Thus from this point of view plastic deformation seems unlikely. However, in the absence of further experiments this question remains unanswered.

3.4. Surface morphology

An estimate of the flaw size, a, can be made from knowledge of σ_f and K_{1c} [26] using the equation

$$K_{1c} = \frac{Y}{Z}\,\sigma_f a^{1/2}.$$

On a number of fracture surfaces the fracture origin could be located at the edge of the surface. It is therefore probable that the flaws are surface flaws. Assuming a semi-circular shape, $Y/Z \sim 1.26$. By using $\sigma_f = 350$ MPa and $K_{1c} = 3.7$ MPa m$^{1/2}$ a value of ~ 70 μm is obtained. From the temperature independence of σ_f and K_{1c} it is clear that the flaw side is temperature independent, unless residual surface stresses due to machining are present.

In order to reveal the possible presence of surface stress, specimens were etched to various depths and the strength at each depth was measured. The results are presented in Fig. 5. The strength is essentially constant with increasing etching depth. Hence only very little or no surface stress is present and the flaw size is indeed temperature independent.

Nevertheless, the surface morphology changes the surface of an as-machined surface of a B_4C specimen shows a regular pattern of damage (Fig. 6). Upon etching the morphology changes gradually until a depth of 30 μm is reached (Fig. 7). Further etching does not change the morphology anymore.

For all etching depths, the Weibull modulus m was again constant at a value of about 5. Since the maximum etching depth (~ 120 μm) is larger than the estimated flaw size (~ 70 μm) and the strength and Weibull modulus are constant, the hypothesis that the flaws are inherent to the material (see Section 3.3) and not due to machining, is further substantiated.

Temperature also has its influence on the sur-

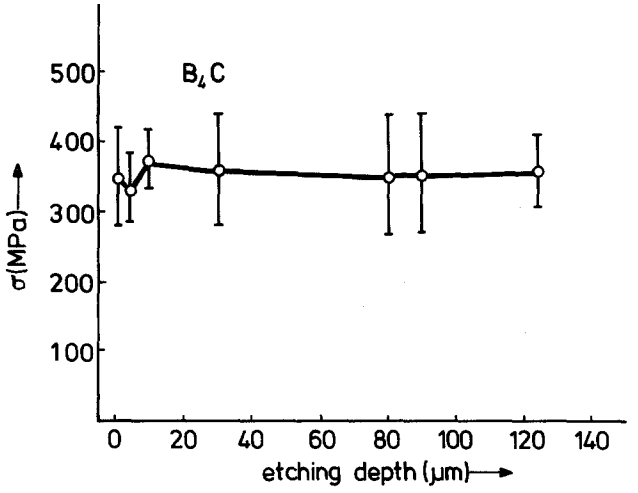

Figure 5 Strength of the B_4C as a function of etching depth. Bars at the data points indicate the sample standard deviation.

face morphology. If the specimen is held at 900 K for 15 min the start of a smoothing process can be seen. After holding the specimen for the same time at 1300 K only the rudiments of the machining damage are observed, while after holding at 1500 K only a smooth surface is left (Fig. 8). The smoothing process is a result of the oxidation of the B_4C, which takes place in spite of the flow of the dry N_2 gas. This has been shown by an XPS analysis of the machined surfaces of specimens fractured at room temperature and 1500 K. A substantial amount of nitrogen is also present in this oxidized layer. Probably the low partial pressure of oxygen is the reason for the formation of a boron oxy-nitride instead of boron oxide.

Since the strength σ_f and the fracture toughness K_{1c} are essentially temperature independent, the smoothed surface layer has no healing effect on the flaws, at least for the relatively short holding time used in this work.

4. Summary and conclusions

The high temperature fracture behaviour of hot-pressed boron carbide has been investigated. The material used was theoretically dense with a grain size of about 10 μm. It was found that the fracture toughness was constant at $\sim 3.7\,\mathrm{MPa\,m^{1/2}}$ up to 1500 K and there was little or no decrease in strength from its room temperature value of ~ 350 MPa. The strength is fairly variable, as reflected by the low Weibull modulus of ~ 5 and probably inherent to the material. Both the order of magnitude and the temperature dependence of the fracture energy, calculated from the fracture toughness and elastic data, can be explained in terms of simple theoretical models using bulk thermal and elastic data.

Acknowledgement

Many thanks are due to Mr Hattu and Mr Parren for their care in carrying out the mechanical experiments.

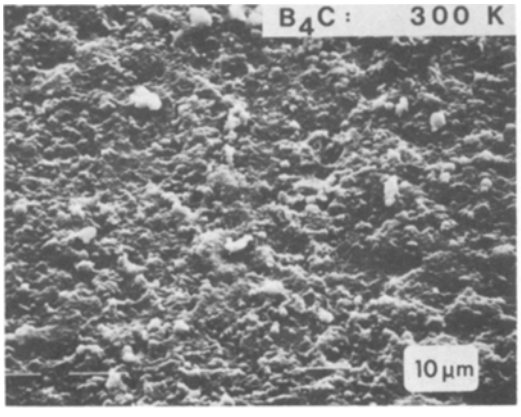

Figure 6 Surface of the B_4C as-machined.

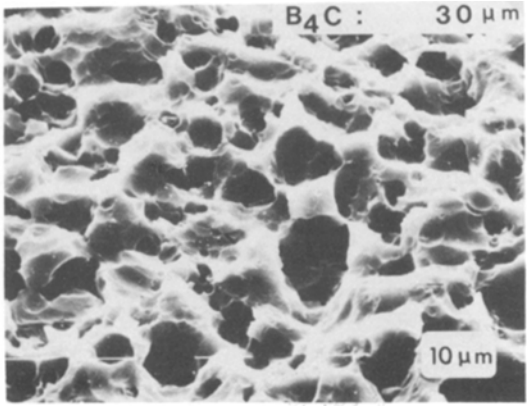

Figure 7 Surface of the B_4C after etching 30 μm.

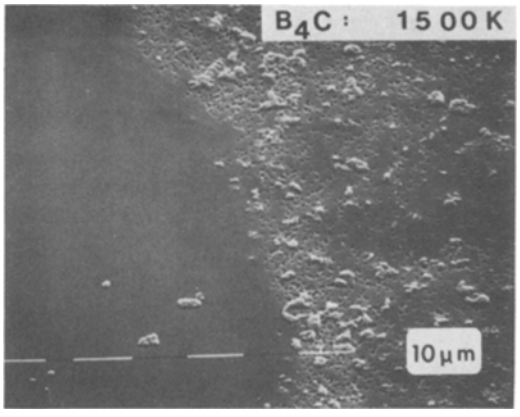

Figure 8 Surface of the B_4C after holding at 1500 K for 15 min.

Appendix I: The bond energy model

For covalently bonded materials an estimate of the fracture energy, γ can be made by counting the number of fractured bonds per unit area and multiplying them by the bond energy [26]. For single crystals the calculation is straight forward, although some ingenuity is necessary for a high index plane [27, 45]. For polycrystalline material an appropriate average has to be calculated, which is not a simple operation. An approximate average, however, may be calculated by using a simple model [28, 29]. For compounds an "average" atom must be used.

The following quantities are defined in advance:

N	Avogadro's constant ($6.023 \times 10^{23}\,\mathrm{mol}^{-1}$)
$V = M/\rho$	molar volume
ρ	density of the material
M	molecular weight
$v = V/N$	volume of the (average) atom
ϕ	(average) bond energy
Z	mean coordination number in the bulk
ΔZ	number of fractured bonds per atom
$a(A)$	total surface area of one (N) atom(s)
$a_s(A_s)$	area of one (N) surface atom(s) exposed to the surface
$a_p(A_p)$	projected area of one (N) surface atom(s)

Now consider one mole of material. Taking into account only nearest neighbour interactions the atomization energy per mole at 0 K, $H(0\,\mathrm{K})$ is given by

$$H(0\,\mathrm{K}) = \frac{N}{2} Z\phi. \tag{A1}$$

In the same approximation

$$\gamma = \frac{\Delta Z\phi}{2a_p} = \frac{\Delta Z H(0\,\mathrm{K})}{ZNa_p} \tag{A2}$$

The factor 1/2 arises from the fact that the fracture process yields two fracture surfaces. In order to calculate γ, the quantities A_p and $\Delta Z/Z$ have to be estimated.

First, consider the estimation of A_p. The polycrystal is simply regarded as a stack of layers containing space filling polyhedra representing the average Wigner–Seitz cell. Miedema [29], in his application of a similar model to metals, takes for the shape of the Wigner–Seitz cell the average of cube and a sphere. The volume V of a cube and sphere are given by:

$$V_{\mathrm{cube}} = a^3, \quad V_{\mathrm{sphere}} = \frac{4\pi r^3}{3} \tag{A3}$$

where a and r are the edge length of the cube and radius of the sphere, respectively. Similarly the total surface A is given by:

$$A_{\mathrm{cube}} = 6a^2, \quad A_{\mathrm{sphere}} = 4\pi r^2. \tag{A4}$$

Accordingly

$$\begin{aligned} A &= (A_{\mathrm{cube}} + A_{\mathrm{sphere}})/2 \\ &= \left(6V_{\mathrm{cube}}^{2/3} + 4\pi\left(\frac{3}{4\pi}\right)^{2/3} V_{\mathrm{sphere}}^{2/3}\right)/2 \\ &= \alpha V^{2/3}, \quad \alpha \approx 5.42. \end{aligned} \tag{A5}$$

The value for α seems a reasonable choice. A similar calculation for the truncated octahedron (or α-tetracaidecahedron) representing the Wigner–Seitz cell in a body centred cubic lattice results in $\alpha \approx 5.35$ [30], while the use of a rhombic dodecahedron, corresponding to a face centred cubic lattice results in $\alpha \approx 5.34$ [30].

The projected area may now be estimated as follows

$$a = f_1 a_s = f_1 f_2 a_p \tag{A6}$$

where f_1 and f_2 are defined by

$$f_1 = a/a_s, \quad f_2 = a_s/a_p. \tag{A7}$$

Since it is assumed that in a fracture surface all possible orientations of the Wigner–Sietz cell are exposed to the surface, the following theorem from stereology may be usefully employed: For a convex body the total surface area, a, is related to the projected surface area, a_p, averaged over all directions [31] by

$$a = 4a_p (= f_1 f_2 a_p). \tag{A8}$$

Hence

$$a_p = a/4 = (\alpha v^{2/3})/4. \tag{A9}$$

Second, consider the estimate for $\Delta Z/Z$. From the stack-of-layers model, one might say that the

TABLE AI Data for B_4C fracture energy calculation

ρ	2520 kg m^{-3}	[16]
M	55.2×10^{-3} kg mol^{-1}	
$V = M/\rho$	2.19×10^{-5} m^3 mol^{-1}	
H (300 K)*	3.14×10^6 J mol^{-1}	[33]

*The difference between H (300 K) and H (0 K) is only minor.

bonds holding each atom are distributed evenly among three planes: the plane of the atom itself and the two neighbouring planes. In this model therefore, on average each plane has a share of 1/3 of the bonds and $\Delta Z/Z = 1/3$. Since for a random distribution of bonds the following relation holds

$$f_1 = a/a_s = Z/\Delta Z \qquad \text{(A10)}$$

it is clear from Equation A8 that either $\Delta Z/Z$ ($= 1/f_1$) or f_2 can be chosen at will, but not both quantities.

The stack-of-layers model with $\Delta Z/Z = 1/3$ has been used before [29, 32]. In [29] an independent estimate for f_2 was made, using a model of irregular dodecahedra like atoms (which incidentally do not yield matching fracture surfaces). The relatively low result $f_2 = 2/3^{1/2} \approx 1.15$ is probably due to the choice of a particular orientation instead of a random one and not consistent with the assumed value of $\Delta Z/Z = 1/3$. It is known that estimates for various surface orientations may differ considerably, e.g. estimates based on the 1 0 0, 1 1 0 and 1 1 1 planes of an array of tetracaidecahedra would result in $f_2 = 1.55$, 1.27 and 1.56, respectively.

Finally, solving for γ gives

$$\gamma = \frac{\Delta Z H(0\,\mathrm{K})}{Z N a_p} = \frac{4}{f_1 \alpha} N^{-1/3} V^{-2/3} H(0\,\mathrm{K})$$
$$\approx 0.25 N^{-1/3} V^{-2/3} H(0\,\mathrm{K})$$
$$(f_1 = 3, \quad \alpha = 5.3) \qquad \text{(A11)}$$

Using the relavant data for B_4C (Table AI) the calculation for the fracture energy yields $\gamma = 11.8$ J m^{-2}.

Appendix II: The "thermal" model

The method as outlined in Appendix I yields a useful estimate of the fracture energy, γ, but, it does not give explicitly the temperature dependence of γ. An interesting way of estimating this dependence is given by the "thermal model" or "method of thermal transformation" ([34], see also [35]).

Assume that one mole of solid is heated from T_1 to T_2 under constant pressure. The internal energy is represented by the sum of the potential energy H (= bond energy) and the kinetic energy L (= vibration energy). From conservation of energy it follows that

$$H(T_2) - H(T_1) + L(T_2) - L(T_1) =$$
$$\int_{T_1}^{T_2} c_p(T)\mathrm{d}T - \int_{T_1}^{T_2} p\left(\frac{\partial V}{\partial T}\right)_p \mathrm{d}T \qquad \text{(B1)}$$

where p is the external pressure, V is the volume of the body and c_p the specific heat at constant pressure.

If the external loads are small, i.e. much less than the theoretical strength, the last term on the right hand side of, e.g. Equation B1, can be ignored. This is equivalent to the usual assumption that the internal energy and the enthalpy are numerically equal to a first approximation. Further it is assumed that the potential energy is much greater than the kinetic energy

$$L(T_1) \ll H(T_1) \qquad \text{(B2)}$$

a condition normally fulfilled if T_1 is low enough. From Equation B1 it then follows that

$$H(T_1) = -\int_{T_1}^{T_2} c_p(T)\mathrm{d}T + L(T_2) + H(T_2) \qquad \text{(B3)}$$

At the boiling point $T_2 = T_b$, $H(T_b) = 0$ while $L(T_b)$ will be equal to the mean kinetic energy of particles at pressure P and temperature T_b. The latter is 3/2 RT_b, according to the kinetic theory of gases. Hence it follows that

$$H(T) = -\int_{T}^{T_b} c_p(T)\mathrm{d}T + \tfrac{3}{2}RT_b. \qquad \text{(B4)}$$

Heat of melting, heat of evaporation and, if present, heat of phase transformations should be included in the first term of the right-hand side of Equation B4. In principle, the value of H (300 K), and hence of γ (see Appendix I), can be calculated from Equation B4. Unfortunately only data for solid B_4C are available.

Fortunately, the temperature dependence of γ can be estimated. Differentiation of Equation A7 yields

$$\frac{1}{\gamma}\left(\frac{\mathrm{d}\gamma}{dT}\right) = \frac{1}{H}\left(\frac{\mathrm{d}H}{\mathrm{d}T}\right) - 2\alpha \qquad \text{(B5)}$$

where α is the linear thermal expansion coefficient. The temperature dependence of H is given by

$$\frac{dH}{dT} = -c_p(T) \qquad \text{(B6)}$$

according to Equation B4.

For B_4C the c_p value is measured up to ~ 1700 K [36, 37] and both references give c_p (300 K) ≈ 54 J mol^{-1} K^{-1}. The α for B_4C is also known [38]: α (300 K) ≈ 4.3 × 10^{-6} K^{-1}. From these data and H (300 K) (see Appendix I) the relative decrease of γ with temperature for B_4C is estimated to be:

$$\frac{1}{\gamma(300\,\mathrm{K})}\left(\frac{d\gamma}{dT}\right) \approx -2.6 \times 10^{-5}\,\mathrm{K}^{-1} \qquad \text{(B7)}$$

Appendix III: The "elastic" model

The "elastic" model described in this appendix has been used to estimate the fracture energy of alkali halides, metals, oxides and covalently bonded materials. It is often attributed to Gilman (e.g. [39]) but in fact Polanyi [40] and Orowan [41] basically used it as early as 1921 and 1934, respectively.

In the model it is assumed that the attractive stress $\sigma(x)$ between two crystal planes can be approximated by a sine function from a_0 (the equilibrium interplanar spacing) up to $a_0 + \lambda$. Here λ is the "range" of the attractive forces.

$$\sigma = \sigma_0 \sin\frac{\pi x'}{\lambda}$$

$$0 < x' \equiv x - a_0 < \lambda. \qquad \text{(C1)}$$

For small displacement from the equilibrium interplanar spacing the material should behave linearly elastic and thus

$$\sin\frac{\pi x'}{\lambda} \simeq \frac{\pi x'}{\lambda} \qquad \text{(C2)}$$

and

$$\sigma = E\left(\frac{x'}{a_0}\right) = \sigma_0\left(\frac{\pi x'}{\lambda}\right) \qquad \text{(C3)}$$

where E is the appropriate Young's modulus. The full expression for the attractive stress is then given by

$$\sigma = \frac{E\lambda}{\pi a_0} \sin\frac{\pi x'}{\lambda}. \qquad \text{(C4)}$$

Now the fracture energy (or in Gilman's terms surface energy) is

$$\gamma = \tfrac{1}{2}\int_0^\infty \sigma(x)dx = \frac{E\lambda}{2\pi a_0}\int_0^\lambda \sin\left(\frac{\pi x'}{\lambda}\right)dx'$$

$$= \frac{E}{a_0}\left(\frac{\lambda}{\pi}\right)^2 \qquad \text{(C5)}$$

The choice of λ largely dictates the extent of agreement that is reached with experiment. Gilman [39] and others [26] state that good agreement between the theoretical and experimental value of surface energy is reached when λ is taken to be equal to the mean radius of the atoms or ions in the surface plane. A more elaborate analysis [42] indicates that the model overestimates γ with a factor of 1.4 to 2, however.

For single crystals the calculation of γ is straight forward. For polycrystalline material, however, it is not clear what choice should be made for λ^2/a_0.

The temperature dependence of K_{1c} can be estimated however, [43] by differentiating formula C5. Assuming λ to be constant, we obtain

$$\frac{1}{\gamma}\left(\frac{d\gamma}{dT}\right) = \frac{1}{E}\left(\frac{dE}{dT}\right) - \frac{1}{a_0}\left(\frac{da_0}{dT}\right) = \frac{1}{E}\left(\frac{dE}{dT}\right) - \alpha. \qquad \text{(C6)}$$

where α is the linear thermal expansion coefficient. The relation between γ and K_{1c} is described by [7]:

$$K_{1c}^2 = 2E\gamma/(1-\nu^2) \qquad \text{(C7)}$$

where ν is Poisson's ratio. Differentiating once more, neglecting the temperature dependence of ν and substituting expression C6 for $1/\gamma\,(d\gamma/dT)$, we have

$$\frac{1}{K_{1c}}\left(\frac{dK_{1c}}{dT}\right) = \frac{1}{E}\left(\frac{dE}{dT}\right) - \tfrac{1}{2}\alpha \qquad \text{(C8)}$$

From the temperature dependence of E [13] and α [38] the relative decrease in γ with temperature for B_4C is estimated to be:

$$\frac{1}{\gamma(300\,\mathrm{K})}\left(\frac{d\gamma}{dT}\right) \approx -1.8 \times 10^{-5}\,\mathrm{K}^{-1}. \qquad \text{(C11)}$$

References

1. A. LIPP, *Technische Rundschau* **14**, 28, **33** (1965) and 7 (1966).
2. D. PROKIC, *J. Phys. D. (Appl. Phys.)* 7 (1974), 1873.
3. M. I. MENDELSON, *J. Amer. Ceram. Soc.* **52** (1969) 443.
4. G. de WITH and N. HATTU, *J. Mater. Sci.* **16** (1981) 841.
5. G. W. HOLLENBERG, G. R. TERWILLIGER and R. S. GORDON, *J. Amer. Ceram. Soc.* **54** (1971) 196.
6. W. F. BROWN and J. R. SRAWLEY, ASTM STP 381 (ASTM, Philadelphia, 1966).

7. R. DAVIDGE, "Mechanical Behaviour of Ceramics", (Cambridge UP, Cambridge, 1979).
8. D. G. S. DAVIES, *Proc. Brit. Ceram. Soc.* **22** (1973) 429.
9. H. F. POLLARD, "Sound Waves in Solids", (Pion Ltd., London, 1977).
10. M. A. KUZENKOVA, P. S. KISLYI, B. L. GRABCHUK and N. I. BODNARUK, *J. Less-Common Met.* **67** (1979) 217.
11. K. H. G. ASHBEE, *Acta Metall.* **19** (1971) 1079.
12. G. W. HOLLENBERG and G. WALTHER, *J. Amer. Ceram. Soc.* **63** (1980) 610.
13. G. W. HOLLENBERG, *Bull. Amer. Ceram. Soc.* **59** (1980) 538.
14. R. S. LIEBLING, *Mater. Res. Bull.* **2** (1967) 1035.
15. J. J. MECHOLSKY Jr, S. W. FREIMAN and R. W. RICE, *J. Mater. Sci.* **11** (1976) 1310.
16. W. H. GUST and E. B. ROYCE, *J. Appl. Phys.* **42** (1971) 276.
17. R. N. KATZ and W. A. BRANTLEY, *Mater. Sci. Res.* **5** (1971) 271.
18. T. VASILOS and S. K. DUTTA, *Bull. Amer. Ceram. Soc.* **53** (1974) 453.
19. K. A. SCHWETZ and W. GRELLNER, *J. Less-Common Met.* **82** (1981) 37.
20. I. A. BAIRAMASHVILI, S. I. KALANDADZE, A. M. ERISTAVI, J. SH. JOBARA, V. V. CHOTULIDI and Yn. I. SALOEV, *J. Less. Common Met.* **67** (1979) 455.
21. C. C. SEATON and S. K. DUTTA, *J. Amer. Ceram. Soc.* **57** (1974), 228.
22. R. W. RICE, *Proc. Brit. Ceram. Soc.* **20** (1972) 205.
23. L. B. EKBOM, *Sci. Ceram.* **9** (1977) 184.
24. J. L. CHERMANT and M. COSTER, *J. Mater. Sci.* **14** (1979) 509.
25. G. de With, *J. Less-Common Met.* accepted.
26. J. M. BLAKELY, "Introduction to the Properties of Crystal Surfaces", (Pergamon Press, Oxford, 1973).
27. A. G. GVOZDEV and L. I. GVOZDEVA, *Phys. Met. Metall.* **31** (1970) 200.
28. W. R. TYSON, *Can. Met. Quart.* **14** (1975) 307.
29. A. R. MIEDEMA, *Z. Metallk.* **69** (1978) 183, 287.
30. J. E. HILLIARD, in "Stereology", Proceedings of the 2nd International Congress for Stereology, edited by H. Elias (Springer, 1967) p. 211.
31. V. VOUK, *Nature* **162** (1948) 330.
32. V. V. OGORODNIKOV and Y. I. ROGOROI, *Sov. Powder Metall.* **1** (1976) 56.
33. D. SMITH, A. S. DWORKIN and E. R. van ARTSDALEN, *J. Amer. Chem. Soc.* **77** (1955) 2654.
34. G. P. CHEREPANOV, "Mechanics of Brittle Fracture", (McGraw-Hill, New York, 1979).
35. V. S. IVANOVA and Y. I. RAGOZIN, *Inorg. Mater.* **1** (1965) 1533.
36. K. K. KELLEY, *J. Amer. Chem. Soc.* **63** (1941), 1137.
37. E. G. KING, *Ind. Eng. Chem.* **41** (1949) 1298.
38. Y. S. TOULOUKIAN (ed), "Thermal Physical Properties of Matter" (IFI/Plenum, New York).
39. J. J. GILMAN, in "Fracture", edited by B. L. Averbach, D. K. Felbeck, G. T. Hahn, and D. A. Thomas, (John Wiley, New York, 1959) p. 193.
40. M. POLANYI, *Z. Phys.* **7** (1921) 323.
41. E. OROWAN, *Z. Krist.* **A89** (1934) 327.
42. N. H. McMILLAN and A. KELLY, *Mater. Sci. Eng.* **10** (1972) 139.
43. R. L. STEWART and R. C. BRADT, *J. Mater. Sci.* **15** (1980) 67.
44. G. K. BANSAL, *J. Amer. Ceram. Soc.* **59** (1976) 87.
45. J. K. McKENZIE, A. J. W. MOORE and J. F. NICHOLAS, *J. Phys. Chem. Solids* **23** (1962) 185.

Received 1 March
and accepted 25 May 1983